Subpicosecond Protein Backbone Changes Detected during the Green-Absorbing Proteorhodopsin Primary Photoreaction

Jason J. Amsden,[†,⊥] Joel M. Kralj,[†,⊥] Logan R. Chieffo,[‡,⊥] Xihua Wang,[†,⊥] Shyamsunder Erramilli,[†,§,⊥] Elena N. Spudich,[||] John L. Spudich,[||] Lawrence D. Ziegler,[‡,⊥] and Kenneth J. Rothschild*[,†,⊥,▽]

Department of Physics, Boston University, Boston, Massachusetts 02215, Department of Chemistry, Boston University, Boston, Massachusetts 02215, Department of Biomedical Engineering, Boston University, Boston, Massachusetts 02215, Center for Membrane Biology, Department of Biochemistry and Molecular Biology, University of Texas Medical School, Houston, Texas 77030, The Photonics Center, Boston University, Boston, Massachusetts 02215, and Department of Physiology and Biophysics, Boston University Medical School, Boston, Massachusetts 02118

Received: May 7, 2007; In Final Form: July 30, 2007

Recent studies demonstrate that photoactive proteins can react within several picoseconds to photon absorption by their chromophores. Faster subpicosecond protein responses have been suggested to occur in rhodopsin-like proteins where retinal photoisomerization may impulsively drive structural changes in nearby protein groups. Here, we test this possibility by investigating the earliest protein structural changes occurring in proteorhodopsin (PR) using ultrafast transient infrared (TIR) spectroscopy with ∼200 fs time resolution combined with nonperturbing isotope labeling. PR is a recently discovered microbial rhodopsin similar to bacteriorhodopsin (BR) found in marine proteobacteria and functions as a proton pump. Vibrational bands in the retinal fingerprint (1175−1215 cm^{-1}) and ethylenic stretching (1500−1570 cm^{-1}) regions characteristic of all-trans to 13-cis chromophore isomerization and formation of a red-shifted photointermediate appear with a 500−700 fs time constant after photoexcitation. Bands characteristic of partial return to the ground state evolve with a 2.0−3.5 ps time constant. In addition, a negative band appears at 1548 cm^{-1} with a time constant of 500−700 fs, which on the basis of total-^{15}N and retinal C15D (retinal with a deuterium on carbon 15) isotope labeling is assigned to an amide II peptide backbone mode that shifts to near 1538 cm^{-1} concomitantly with chromophore isomerization. Our results demonstrate that one or more peptide backbone groups in PR respond with a time constant of 500−700 fs, almost coincident with the light-driven retinylidene chromophore isomerization. The protein changes we observe on a subpicosecond time scale may be involved in storage of the absorbed photon energy subsequently utilized for proton transport.

Introduction

Proteorhodopsin (PR), a newly discovered microbial rhodopsin found in marine proteobacteria, functions as a light-driven proton pump[1,2] similar to bacteriorhodopsin (BR). Over 4000 different PR variants have been discovered that are distributed throughout the world's oceans.[3−5] PR-containing bacteria account for ∼13% of the microorganisms in the oceans' photic zone and are responsible for a significant fraction of the biosphere's solar energy conversion.[2,6] Similar to BR and other microbial rhodopsins, PR consists of seven transmembrane α-helices containing a retinylidene chromophore covalently bound to a lysine (Lys-231) via a protonated Schiff base.[1] Light absorption by PR results in an all-trans to 13-cis isomerization of the retinal which then drives a series of reaction steps taking a total of approximately 20 ms that result in a proton being pumped from the cytoplasm to the extracellular medium.[7]

Recent ultrafast visible absorption experiments[8,9] indicate that the primary photoreaction in PR occurs on a similar time scale (∼0.5 ps) to BR.[10−12] However, visible absorption studies only probe the electronic state of the chromophore. In contrast, IR difference spectroscopy can directly detect small changes occurring in all the molecular components of proteins.[13] Low-temperature (80 K) Fourier transform infrared (FTIR) difference spectroscopy detects changes occurring in the conformation of the chromophore, protein, and internal water molecules of a green-absorbing PR (GPR) during the GPR → K phototransition.[14] However, measurements on cryogenically trapped intermediate states may not accurately reflect native structural changes occurring in PR and other proteins on ultrafast time scales at room temperature (RT = 298 K).

Recent ultrafast transient infrared (TIR) studies on photoactive proteins such as photoactive yellow protein,[15] myoglobin,[16] and green fluorescent protein[17] demonstrate that proteins can react within several picoseconds to nanoseconds following photon absorption by their chromophores. UV resonance Raman spectroscopy on rhodopsin[18] and ultrafast TIR measurements on the related archaeal microbial rhodopsins BR,[10] sensory rhodopsin II (SRII),[19] and halorhodopsin (HR)[20] all suggest that protein responses may occur even faster, and may be coincident with the initial subpicosecond all-*trans*- to 13-*cis*-retinal isomer-

* Corresponding author. E-mail: kjr@bu.edu.
† Department of Physics, Boston University.
‡ Department of Chemistry, Boston University.
§ Department of Biomedical Engineering, Boston University.
|| University of Texas Medical School.
⊥ The Photonics Center, Boston University.
▽ Boston University Medical School.

10.1021/jp073490r CCC: $37.00
Published on Web 09/19/2007

ization. However, these conclusions are limited by instrument response (~1 ps) in the case of rhodopsin[18] or rest on the appearance of bands which may arise from either chromophore or protein vibrations.[10,19,20]

We report here for the first time ultrafast TIR studies with ~200 fs time resolution at RT over the first 30 ps of the photocycle of a green-absorbing proteorhodopsin (GPR) variant found in marine proteobacteria from Monterey Bay strain EBAC 31A8. Measurements were made in the 1500−1570 cm^{-1} region characteristic of retinylidene ethylenic C═C stretching normal modes and the amide II mixed mode involving the C−N stretch and C−N−H bend of peptide groups, and in the 1175−1215 cm^{-1} C−C stretch fingerprint region which is sensitive to the retinal chromophore configuration.[21,22] Here, using ultrafast TIR spectroscopy with subpicosecond time resolution combined with protein and chromophore isotope labeling, we identify chromophore and protein vibrations in GPR and find that an amide II protein backbone vibration undergoes a frequency downshift with a time constant of 500−700 fs, coincident with retinal chromophore isomerization.

Experimental Methods

Protein Expression and Purification. Procedures for protein expression and purification were described previously.[23] *E. coli* cells containing the GPR-encoding plasmid (Monterey Bay strain EBAC 31A8) were cultured on standard Luria Broth medium (Sigma Aldrich) and supplied with either all-*trans*-retinal or all-*trans*-retinal containing a deuterium on carbon 15 (C15D). Total-^{15}N labeling was achieved by growing *E. coli* containing the GPR-encoding plasmid on isotopically labeled growth media (Bioexpress Cell Growth Media, U-15N, 98%, Cambridge Isotope Laboratories, Inc.). After the induction period, the cells expressing His-tagged wild-type GPR were centrifuged at 1000*g*, resuspended in 5 mM $MgCl_2$, 150 mM Tris·HCl, pH 7.0, and disrupted by sonication. The membranes containing pigment were collected by centrifugation (39000*g*, 60 min) and solubilized in a wash buffer (50 mM potassium phosphate, 300 mM NaCl, 5 mM imidazole, and 1.5% octylglucoside (OG), pH 7.0) for at least 1 h at 4 °C. Unsolubilized membranes were removed by centrifugation at 28000*g* for 30 min. The supernatant was incubated with a His-binding resin on a shaker at 4 °C for at least 1 h. The bound resin was applied to a 10 cm chromatography column and washed with 3× volume of wash buffer followed by elution buffer (50 mM KP*i*, 300 mM NaCl, 250 mM imidazole, and 1.0% OG, pH 7.0). The sample purity was assessed by UV−visible spectroscopy.[1]

Proteoliposome Reconstitution. Purified His-tagged GPR was reconstituted into *E. coli* polar lipids (Avanti, Alabaster AL) at a 1:10 protein-to-lipid (w/w) ratio. Lipids initially dissolved in chloroform were dried under argon and resuspended in the dialysis buffer (50 mM potassium phosphate, 300 mM NaCl, pH 7.0) to which OG was added to the final concentration of 1%. The lipid solution was incubated with the OG-solubilized protein for 1 h on ice and dialyzed against the dialysis buffer with three buffer changes every 24 h. The reconstituted protein was centrifuged for 15 min and resuspended in the sample buffer (50 mM CHES, 150 mM NaCl, pH 9.5).

Sample Preparation. For ultrafast TIR measurements, the reconstituted protein was suspended in sample buffer (50 mM CHES, 150 mM NaCl, pH 9.5) and then pelleted in an Eppendorf tube at 14 000 rpm for 20 min. After centrifugation, the excess buffer was removed and the pellet was pressed between two 32 mm × 3 mm circular CaF_2 windows separated by a 25 μm Teflon spacer. The visible absorption maximum for the samples was approximately 0.2 OD (OD = Optical Density) at 520 nm. During experiments, the samples were rotated and translated perpendicular to the laser beams in order to provide a fresh area of sample for each laser shot using an apparatus similar to that described previously.[24] We found that liquid samples resulted in more spatially homogeneous samples and consequently better signal/noise transient signals than hydrated films. This method also provided better sample pH control, which is required due to the strong pH dependence on the dynamics of photoisomerization.[8,9] In addition, the sample holder was kept at 298 K using a circulating water bath.

Pump−Probe Spectrometer. The visible-pump infrared-probe spectroscopy apparatus is based on a commercial Spectra Physics Hurricane Ti:sapphire regenerative amplifier and two Spectra Physics optical parametric amplifiers (OPAs): Models 800 and 800C. The Hurricane amplifier produces 1 mJ laser pulses with ~130 fs duration at 1 kHz repetition rate and a wavelength of 800 nm. The pulses from the amplifier are split by a 50/50 beamsplitter and used to pump the two OPAs. Both OPAs employ two-stage amplification and frequency conversion of the pump pulses from the Hurricane in a type II BBO crystal to produce tunable signal and idler laser pulses from 1.1−1.6 and 1.6−3.0 μm, respectively. In the OPA 800C, difference frequency mixing of the signal and idler laser pulses in a $AgGaS_2$ crystal produces tunable mid-IR laser pulses from 3.0 to 10 μm with spectral full width at half-maximum of ~100−150 cm^{-1}. A small portion (estimated at ~100 nJ/pulse) of this IR light was directed through the sample. The mid-IR laser pulse optical path is purged with dry air to avoid absorption from water vapor. In the second OPA, sum frequency generation of the signal and residual 800 nm pump in a type I BBO crystal produces laser pulses at 520 nm. Samples were excited with 100 nJ 520 nm visible pulses.

The pulses from the two OPAs were parallel polarized and overlapped at the sample in a noncollinear ~11° geometry. The IR beam was approximately 300 μm in diameter, while the visible beam was kept slightly larger (~400 μm). After the sample, the mid-IR pulses are directed into a spectrometer and dispersed onto a 32 element mercury cadmium telluride linear array detector (Infrared Associates, Inc.). Visible pulses are sent through a variable optical delay and chopped at half the repetition of the mid-IR pulses. This results in a transient absorbance difference between pumped and unpumped sample at a delay time between the visible and mid-IR laser pulses. Boxcar integration and digitization of the detector response is performed by a multichannel laser pulse spectroscopy system from Infrared Systems Development Corp. and Labview software. The cross correlation of the visible and IR pulses was determined by measuring photoinduced reflectivity in a 100 μm thick silicon wafer. The cross correlation indicates a system response of ~180 fs near the ethylenic region (1570−1500 cm^{-1}) and ~250 fs near the fingerprint region (1215−1175 cm^{-1}).[25,26] This also provides a measure of time zero for the system with a precision of ~50 fs.

Data Collection and Analysis. At each time delay, the signal was accumulated for 20 s and the results for six or more scans were averaged. The GPR preparation used is very sensitive to photobleaching by the exciting laser, so at various times during the scan the signal at $t = 0$ was collected. Using these data points, the entire set was normalized for the loss of population due to photobleaching similar to previous visible absorption experiments on GPR.[27] At the end of data collection (8−10 h) the signal was ~2 times smaller than at the beginning of the scan. In addition, spectra were taken with 10, 30, 50, 70, 90,

and 110 nJ/pulse showing a linear increase in signal size with excitation power and otherwise identical spectra. See the Supporting Information (SI) Figure S1 for a comparison of transient difference spectra taken at various delay times for 30 and 100 nJ excitation.

A global analysis was performed on the data using Wavemetrics Igor Pro version 5.05A. Transient signals were fit to eq 1, where the pump induced absorbance changes are modeled

$$\Delta A(\nu_{\text{probe}},t) = A_{\text{long}}(\nu_{\text{probe}}) + \sum_{i=1}^{N} A_i(\nu_{\text{probe}})\mathrm{e}^{-(t/\tau_i)} \qquad (1)$$

by a sum of two or three exponentials plus an absorbance change at long (>30 ps) delay times, $A_{\text{long}}(\nu_{\text{probe}})$, which evolves on a time scale longer than ~100 ps. This procedure resulted in decay associated spectra (DAS) $A_i(\nu_{\text{probe}})$ and their corresponding time constants τ_i for the exponential decay rates.[28] Signals at early (<200 fs) delay times are partly obscured by contributions from the free induction decay induced by the probe pulse and perturbed by the pump pulse;[29] therefore, we restricted our analysis to the observed signals at delay times >150 fs in the ethylenic and >200 fs in the fingerprint regions.

Results

Figures 1, 2, 4, and 5 show the TIR spectra for the ethylenic and fingerprint regions of GPR for labeled and unlabeled samples and Figure 3 shows a comparison of unlabeled and total-^{15}N labeled GPR in the ethylenic region at four delay times. The top panel in Figures 1, 2, 4, and 5 is a two-dimensional surface plot representing the temporal evolution of the TIR spectra, where red represents a positive absorbance change and blue represents a negative absorbance change. The bottom panel in each figure displays TIR spectra at various delay times. Negative bands correspond to vibrations in the ground state of GPR removed by photoexcitation, while positive bands result from the IR absorption of transient photoproducts at different time delays between the visible pump and infrared probe pulses.

Ethylenic Region. In the ethylenic region (Figure 1), a negative band appears at 1536 cm^{-1} within the time resolution of the apparatus that decreases in amplitude and shifts to higher frequency (1538 cm^{-1}) at later times due to overlap with the transient absorption of photoproduct bands. A positive peak near 1519 cm^{-1} begins to appear in the first picosecond and shows relatively little change after 3 ps. A negative band at 1548 cm^{-1} also begins to appear in the first picosecond and is most evident at later times (>3 ps). On the basis of an empirical inverse relationship between the visible absorption maximum and the ethylenic stretching frequency established for rhodopsin[30] and later observed in bacteriorhodopsin,[31] the 1536 cm^{-1} band is assigned to the ground state ethylenic vibration of the retinal chromophore in GPR absorbing near 523 nm and the 1519 cm^{-1} positive band to a red-shifted K-like intermediate characteristic of the primary photoproduct in all microbial rhodopsins. The TIR spectrum at 30 ps resembles the static GPR → K FTIR difference spectrum obtained at low temperature (80 K)[14] (dashed line, Figure 1a), with the exception of the negative band near 1548 cm^{-1}.

In order to assign the 1548 cm^{-1} band, we expressed GPR using total-^{15}N isotopically labeled growth media or with all-*trans*-retinal containing a deuterium on carbon 15 (C15D). These labels facilitate assignment of vibrational modes but are not expected to alter protein or chromophore structure or structural changes. Consistent with earlier studies,[32,33] total-^{15}N labeling causes a downshift of 14 cm^{-1} in the amide II normal mode in

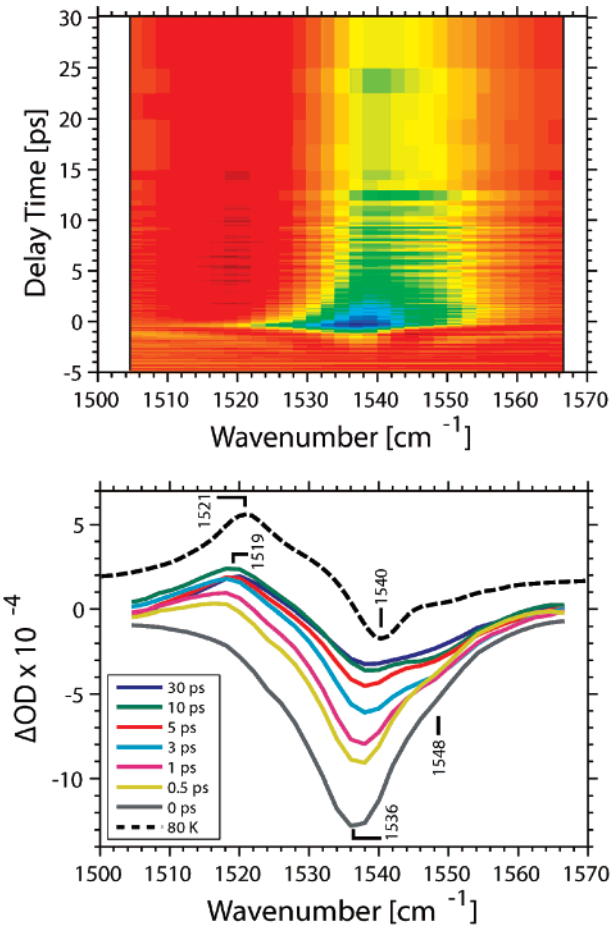

Figure 1. Transient infrared spectrum of unlabeled GPR in the ethylenic (1570−1500 cm^{-1}) region after ~100 nJ 520 nm photoexcitation. (top) Color representation of the temporal evolution of the TIR spectra, where red represents positive absorbance change and blue represents negative absorbance change. (bottom) Transient spectra at various delay times compared to the low-temperature FTIR difference spectrum from ref 14. The dotted lines representing the 80 K FTIR difference spectrum are offset by 2 × 10^{-4} OD for clarity. ΔOD = absorbance change.

the GPR FTIR absolute absorption spectrum (see SI Figure S2). However, this label does not alter retinal ethylenic normal modes of GPR as shown by resonance Raman spectroscopy (RRS) (see SI Figure S3) even though a ^{15}N label is incorporated into the Schiff base through the attached lysine. In contrast, consistent with earlier studies[21] C15D retinal labeling downshifts the main ethylenic mode ~5 cm^{-1} in the RRS of GPR (see SI Figure S3). Since the C15D label is only incorporated into the chromophore, it should not alter protein vibrations as confirmed by low-temperature FTIR difference spectra of GPR[14] (data not shown).

Figure 2 displays the TIR spectra for total-^{15}N labeled GPR in the ethylenic region. Similar to unlabeled GPR, a negative band appears at 1536 cm^{-1} within the time resolution of the apparatus which then decreases in amplitude and shifts to higher frequency (1538 cm^{-1}) at later times due to overlap with photoproduct bands and is assigned to the ground state ethylenic vibration. Also, a positive peak near 1519 cm^{-1} begins to appear in the first picosecond with relatively little change after 3 ps and is assigned to the red-shifted photoproduct. Figure 3 shows a comparison of the unlabeled and total-^{15}N labeled TIR spectra at four delay times. The negative band at 1548 cm^{-1} is significantly more negative in amplitude in each of the unlabeled spectra, except at $t = 0$ where the labeled and unlabeled spectra

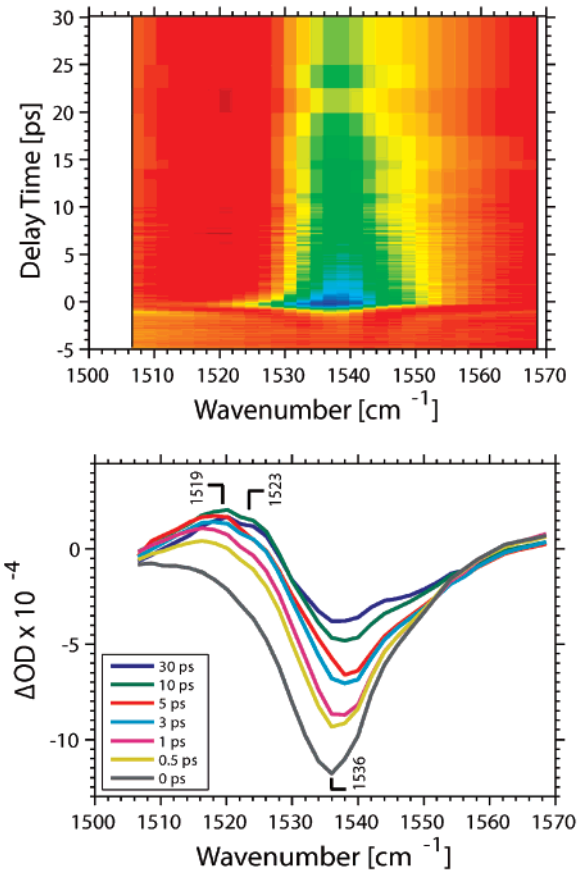

Figure 2. Transient infrared spectrum of total-^{15}N labeled GPR in the ethylenic (1570−1500 cm^{-1}) region after ∼100 nJ 520 nm photoexcitation. (top) Color representation of the temporal evolution of the TIR spectra, where red represents positive absorbance change and blue represents negative absorbance change. (bottom) Transient spectra at various delay times. ΔOD = absorbance change.

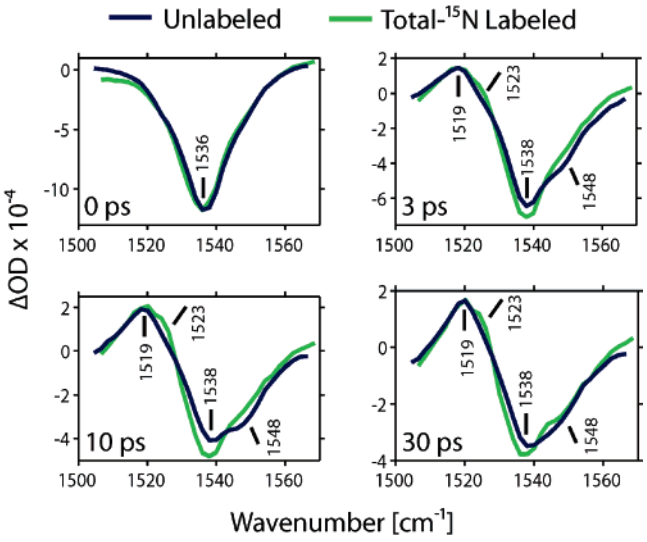

Figure 3. Transient infrared spectra comparing unlabeled (blue trace) and total-^{15}N labeled (green trace) GPR at 0, 3, 10, and 30 ps after 100 nJ photoexcitation at 520 nm in the 1570−1500 cm^{-1} region of the infrared spectrum. ΔOD = absorbance change.

are very similar. The gradual appearance of this negative band in unlabeled GPR with a time constant of 500−700 fs (see below) is consistent with its assignment to an amide II mode which undergoes a change in frequency and/or intensity and not to a retinal ethylenic mode in the ground state of GPR which

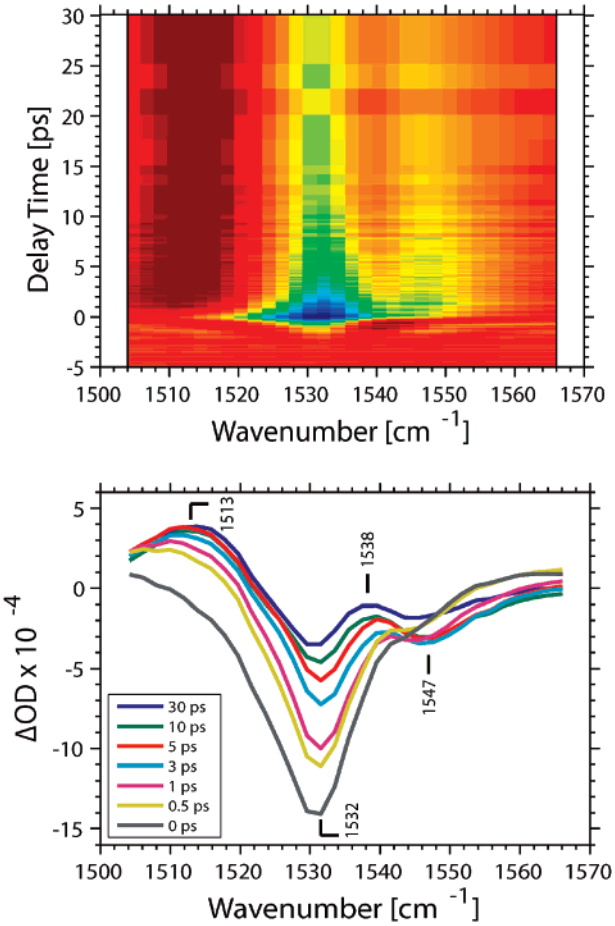

Figure 4. Transient infrared spectrum of C15D retinal labeled GPR in the ethylenic (1570−1500 cm^{-1}) region after ∼100 nJ 520 nm photoexcitation. (top) Color representation of the temporal evolution of the TIR spectra, where red represents positive absorbance change and blue represents negative absorbance change. (bottom) Transient spectra at various delay times. ΔOD = absorbance change.

is expected to result in a negative band at $t = 0$. Furthermore, the expected ∼14 cm^{-1} downshift of this band in the total-^{15}N label would result in partial overlap with the 1538 cm^{-1} ethylenic stretch mode, thus explaining the observed increase in negative absorbance near this frequency in the total-^{15}N labeled vs unlabeled spectra after $t = 0$ (Figure 3). In addition, the positive band appearing at 1523 cm^{-1} in the total-^{15}N label may indicate a ∼14 cm^{-1} downshift of a hidden positive amide II band which overlaps with the 1538 cm^{-1} peak in the unlabeled GPR.

In GPR containing C15D labeled retinal, (Figure 4) the ethylenic bands at 1536 and 1519 cm^{-1} downshift ∼5 cm^{-1}, further confirming the presence of an unshifted negative band near 1547 cm^{-1} appearing with a 500−700 fs time constant (see below). In addition, an apparent positive band is seen near 1538 cm^{-1} which is at the predicted position to explain the positive 1523 cm^{-1} band in the total-^{15}N label (see above). The combination of the isotope labeling of the protein and retinal thus confirms the assignment of these bands to the downshift of an amide II mode from 1548 cm^{-1} to near 1538 cm^{-1} in less than a picosecond after photoexcitation. Note that a small residual band at 1548 cm^{-1} still remains at $t = 0$ in the C15D TIR spectrum (Figure 4). Since this band is also seen as a small shoulder at the same frequency in the $t = 0$ TIR spectra as well as the RRS of GPR independent of C15D and total-^{15}N labeling (see SI Figure S3), it most likely corresponds to a nonfunda-

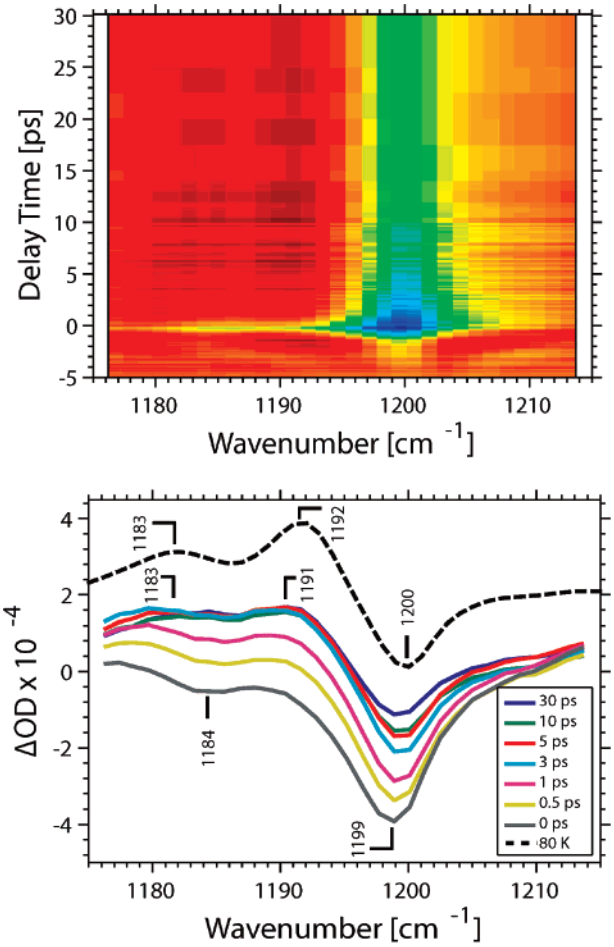

Figure 5. Transient infrared spectrum of unlabeled GPR in the retinal fingerprint (1215−1175 cm^{-1}) region after ~100 nJ 520 nm photoexcitation. (top) Color representation of the temporal evolution of the TIR spectra, where red represents positive absorbance change and blue represents negative absorbance change. (bottom) Transient spectra at various delay times compared to the low-temperature FTIR difference spectrum from ref 14. The dotted lines representing the 80 K FTIR difference spectrum are offset by 2×10^{-4} OD for clarity. ΔOD = absorbance change.

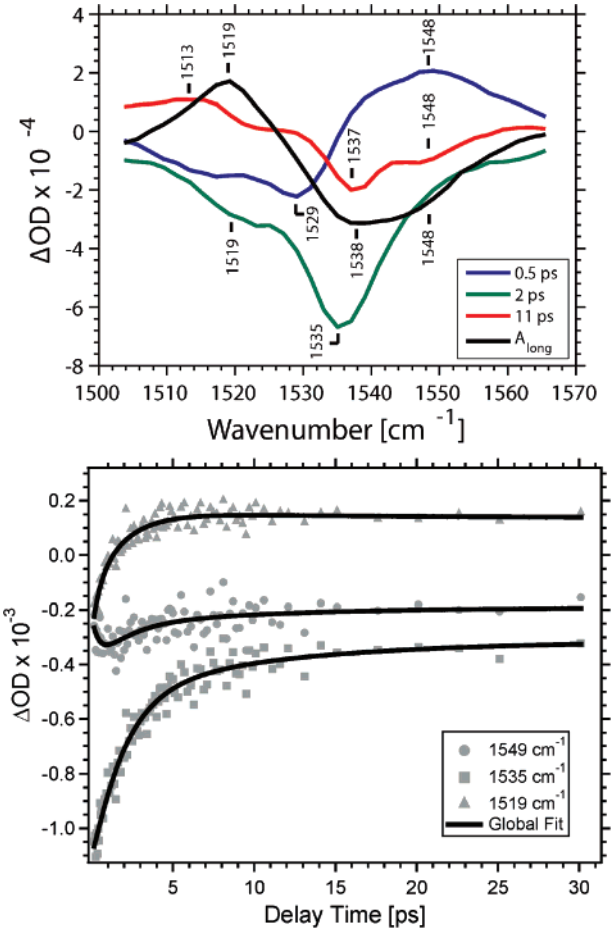

Figure 6. (top) DAS for unlabeled GPR resulting from a triple exponential global fit in the 1570−1500 cm^{-1} region of the infrared spectrum for time constants of 0.5, 2, and 11 ps. The constant trace refers to the transient difference spectrum at long delay times, >30 ps in our experiment. (bottom) Experimental data points plotted at selected frequencies along with the results of a triple exponential global fit with time constants of 0.5, 2, and 11 ps. ΔOD = absorbance change.

mental mode observed at the same frequency in the RRS of the related protein BR.[21]

Fingerprint Region. In the 1175−1215 cm^{-1} fingerprint region (Figure 5), negative bands appear at 1199 and 1184 cm^{-1} within the time resolution of our apparatus, and decrease in amplitude at later times. In addition, two positive bands appear at 1191 and 1183 cm^{-1} with a time constant of approximately 700 fs (see below). The TIR spectra obtained at 30 ps closely resemble the static low-temperature FTIR difference spectrum of GPR (dashed line, Figure 1b).[14] The 1199 and 1184 cm^{-1} negative bands are assigned to the C−C stretch of the all-*trans*-retinylidene chromophore, and the positive 1191 and 1183 cm^{-1} bands correspond to the 13-cis configuration on the basis of comparison to RRS of BR and low-temperature FTIR of GPR.[14,21,22,34]

Kinetic Analysis. To analyze the kinetics of the structural changes observed in GPR, global analysis was performed to derive time constants and DAS (see Experimental Methods). Figures 6−8 show the DAS for the unlabeled, retinal C15D labeled, and total-^{15}N labeled GPR in the ethylenic region, respectively. Figure 9 shows the DAS for unlabeled GPR in the fingerprint region. In Figures 6−9, the top panel displays the DAS $A_i(\nu_{probe})$ for the two or three time constants as well as $A_{long}(\nu_{probe})$ representing the pump induced transient spectrum at long delay times (>30 ps). The bottom panel shows the time evolution of the signal at selected frequencies along with the global exponential fit. Overall, the kinetic analysis yields three time constants including a subpicosecond (500−700 fs) time constant indicating isomerization of the chromophore and perturbation of the amide II normal mode, a slower 2−3.5 ps time constant indicating a parallel path from the excited state back to the all-trans form of the chromophore as well as a sequential J−K-like transition as seen in BR,[10,36] and a long ~11 ps time constant indicating relaxation of the amide II perturbation and possible minor structural rearrangements of the chromophore in the resulting all-trans and 13-cis forms. Figure 10 displays a reaction scheme based on our interpretation of the DAS. The dotted lines in Figure 10 represent processes deduced by previous visible[8,9,35] and FTIR[7,35] experiments but not measured in this experiment due to our time resolution (~0.2 ps) and the time scales over which we measured (0.2−30 ps), while the solid lines indicate states deduced from our TIR data.

In the ethylenic region for unlabeled GPR, a band appears at 1529 cm^{-1} in the 500 fs DAS (Figure 6, blue trace). This band corresponds to the 1519 cm^{-1} peak assigned to the ethylenic mode of the red-shifted photoproduct observed in the TIR spectrum (Figure 1). This band appears at a higher frequency in the DAS due to the absence of the negative band at 1536 cm^{-1} in the TIR spectra which causes band splitting.[14] As

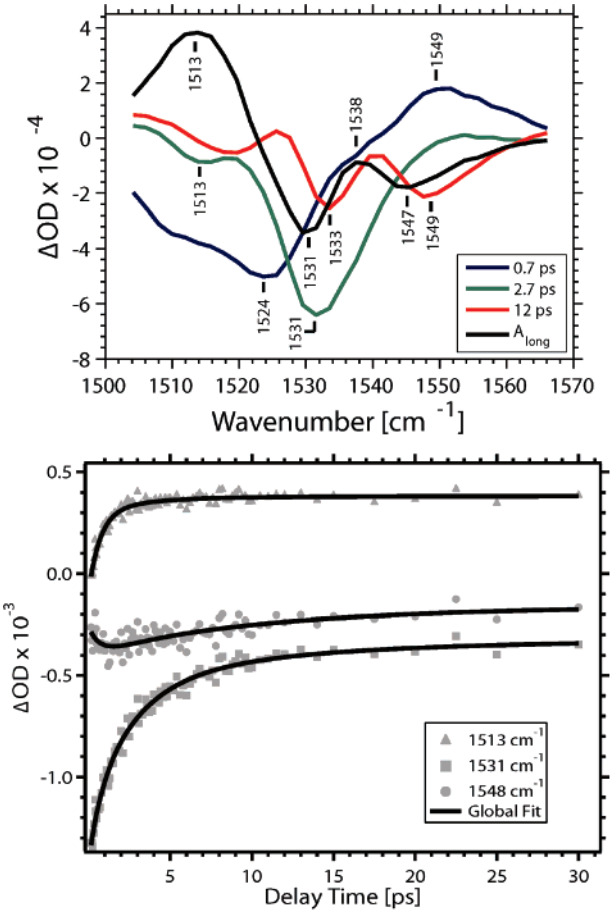

Figure 7. (top) DAS for C15D retinal labeled GPR resulting from a triple exponential global fit in the 1570−1500 cm^{-1} region of the infrared spectrum for time constants of 0.7, 2.7, and 12 ps. The constant trace refers to the transient difference spectrum at long delay times, >30 ps in our experiment. (bottom) Experimental data points plotted at selected frequencies along with the results of a triple exponential global fit with time constants of 0.7, 2.7, and 12 ps. ΔOD = absorbance change.

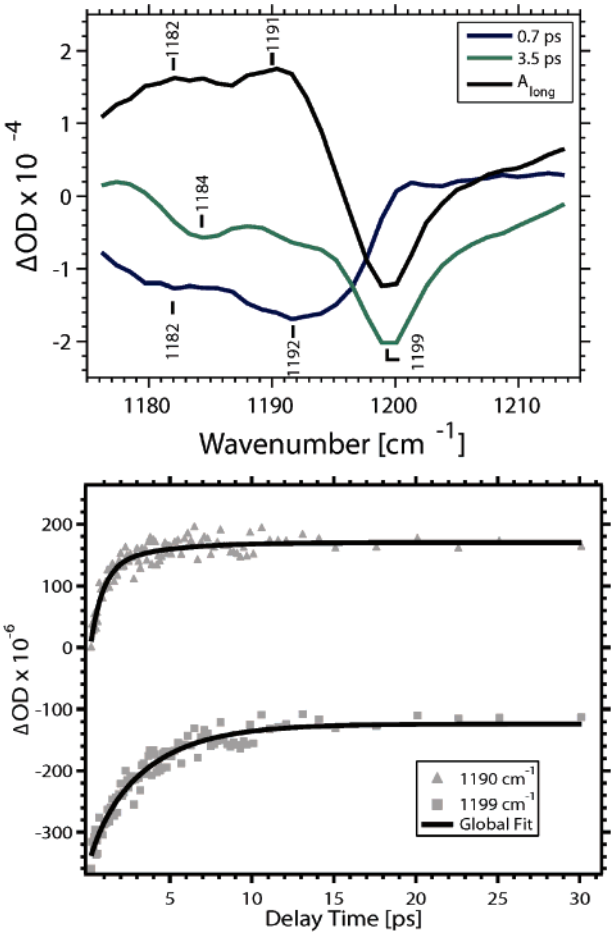

Figure 8. (top) DAS for unlabeled GPR resulting from a double exponential global fit in the 1215−1175 cm^{-1}region of the infrared spectrum for time constants of 0.7 and 3.5 ps. The constant trace refers to the transient difference spectrum at long delay times, >30 ps in our experiment. (bottom) Experimental data points plotted at selected frequencies along with the results of a triple exponential global fit with time constants of 0.7 and 3.5 ps. ΔOD = absorbance change.

expected, this band downshifts ∼5 cm^{-1} to 1524 cm^{-1} in the 700 fs DAS of the C15D labeled GPR (Figure 7, blue trace). The band near 1548 cm^{-1} assigned to the amide II vibration also appears in the fast 500−700 fs time constant DAS in both unlabeled and C15D labeled GPR (Figure 6 and 7, blue traces), indicating that this protein structural change occurs concomitantly with formation of the 13-*cis*-retinal photoproduct. In the total-^{15}N labeled GPR there is no evidence of a band at 1548 cm^{-1} in the fast 700 fs DAS or in the DAS for any of the other time constants (Figure 9). The C−C retinal fingerprint bands at 1191 and 1183 cm^{-1} associated with formation of the 13-*cis*-retinal configuration also appear with a similar fast time constant (700 fs) (Figure 8, blue trace), indicating that an all-trans to 13-cis isomerization occurs on this time scale.

In contrast to the fast formation of the 13-cis photoproduct from the excited state, a parallel partial repopulation of the ground state from the excited state occurs as evidenced by the decreasing amplitude of the 1536, 1199, and 1184 cm^{-1} bands assigned to the ground state ethylenic and fingerprint modes in unlabeled GPR (Figures 1 and 5). Bands near 1535, 1199, and 1184 cm^{-1} in the 2 and 3.5 ps DAS for unlabeled GPR in the ethylenic and fingerprint regions, respectively (Figures 6 and 9, green traces), indicate a slower time constant for this partial repopulation of the ground state. A similar 2.7 ps time constant is associated with the partial recovery of the C15D isotope shifted ground state ethylenic mode at 1532 cm^{-1} in GPR containing C15D labeled retinal (Figure 7, green trace). Additionally, a band appears near 1519 cm^{-1} in the unlabeled GPR 2 ps DAS. This band shifts to near 1514 cm^{-1} in the retinal C15D labeled GPR. This indicates a transition similar to the 3 ps J−K transition observed in BR[10,36] and attributed to vibrational cooling and torsional relaxation of the retinal. However, a 3 ps process representing a J−K-like transition was not observed in the ultrafast visible experiments on PR.[8,9]

Spectral changes near 1548 cm^{-1} evolving with an 11−12 ps time constant seen in the long time constant DAS for unlabeled and C15D retinal labeled GPR (Figures 6 and 7, red traces) reflect relaxation of the amide II perturbation. Additional spectral changes in the 11−12 ps DAS for unlabeled and C15D retinal labeled GPR may indicate further rearrangements of the chromophore or a second slower decay from the excited state evident in ultrafast visible absorption measurements.[8,9] In particular, a band appears near 1537 cm^{-1} in the 11 ps DAS for unlabeled GPR. This band shifts ∼5 cm^{-1} to near 1532 cm^{-1} in the C15D labeled retinal, possibly indicating further repopulaton of the all-trans state. Also, a band at 1513 cm^{-1} in the 11 ps DAS for unlabeled GPR appears to downshift outside our detection window in the DAS for C15D retinal labeled GPR, possibly indicating some rearrangement of the 13-cis chromophore.

The total-^{15}N labeled GPR has a 7.2 ps time constant related to the partial recovery of the ground state at 1538 cm^{-1} (Figure

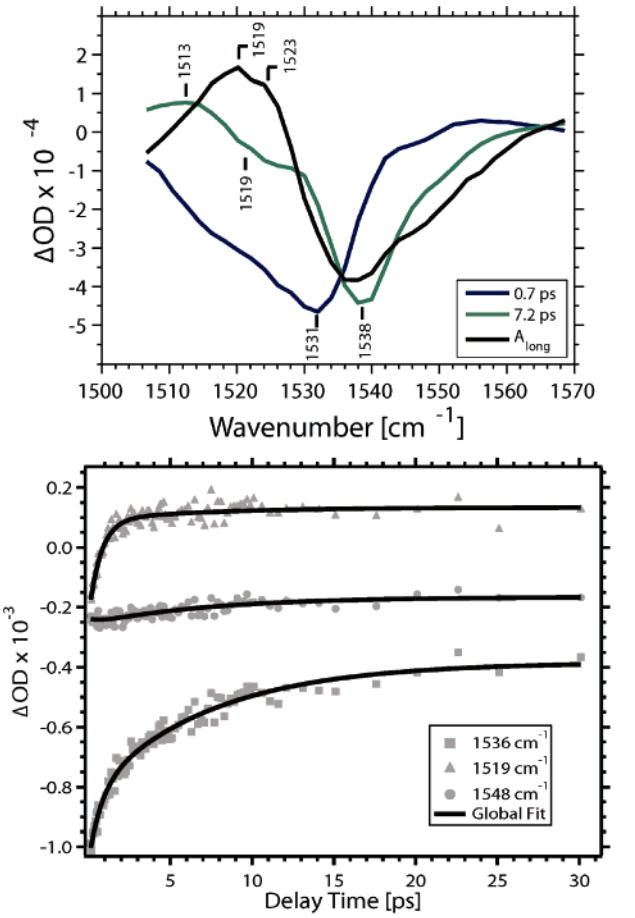

Figure 9. (top) DAS for total-^{15}N labeled GPR resulting from a double exponential global fit in the 1570−1500 cm^{-1} region of the infrared spectrum for time constants of 0.7 and 7.2 ps. The constant trace refers to the transient difference spectrum at long delay times, >30 ps in our experiment. (bottom) Experimental data points plotted at selected frequencies along with the results of a triple exponential global fit with time constants of 0.7 and 7.2 ps. ΔOD = absorbance change.

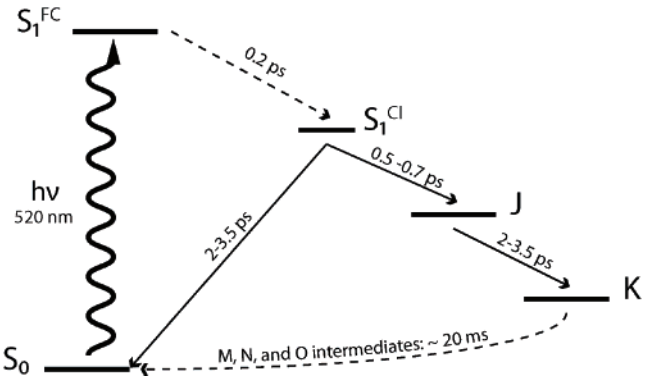

Figure 10. Kinetic scheme for the GPR primary photoreaction based upon TIR data and previous visible[8,9,35] and FTIR[7,35] experiments. Dotted lines indicate processes not measured due to our time resolution (~0.2 ps) or to the time scales over which we measured (0.2−30 ps), while solid lines indicate processes deduced from our data. S_0 indicates the all-trans ground state of the protein, while S_1^{FC} and S_1^{CI} represent the Franck−Condon region and conical intersection of the retinal excited state, respectively. J and K represent the red-shifted 13-cis photointermediates.

8, green trace). The length of this time constant compared to those in unlabeled and C15D labeled GPR may be due to overlapping signals unresolved by global fitting. These overlapping signals are likely due to ground state recovery, amide II relaxation, and additional rearrangements of the chromophore and protein groups as seen in unlabeled and C15D labeled GPR with an 11−12 ps time constant. For example, the 7.2 ps DAS for total-^{15}N labeled GPR exhibits bands at 1538 and 1519 cm^{-1} similar to bands at 1537 and 1519 cm^{-1} in the unlabeled GPR 2 ps DAS attributed to partial repopulation of the ground state and a J−K-like transition, as well as a band at 1513 cm^{-1} found in the 11 ps DAS for unlabeled GPR, possibly indicating further minor structural changes in the retinal.

Discussion

The TIR data indicate that the early events occurring in GPR are similar to those in BR based on ultrafast Raman,[37] visible absorption,[11,12,38,39] and TIR[10] studies and are consistent with visible absorption experiments[8,9] as discussed below. In BR, visible photon absorption produces an excited state with all-*trans*-retinal which decays in approximately 500 fs to a red-shifted J-intermediate with a 13-*cis*-retinal configuration or returns with a 1 ps time constant to the all-trans configuration. Then, in ~3 ps the K-intermediate forms from the 13-cis species through vibrational cooling and torsional relaxation of the retinal.

In GPR, TIR data indicate that absorption of a photon results in an all-*trans*- to 13-*cis*-retinal chromophore isomerization and formation of a red-shifted photointermediate with a 500−700 fs time constant. Partial relaxation back to the ground state from the excited state along with a J−K-like transition in the photoproduct occurs on a slower 2.0−3.5 ps time scale (see Figure 10). Subpicosecond visible absorption studies of PR reconstituted in halobacterial lipids at pH 9.0 revealed three time constants of <200 fs, 400 fs, and 8 ps.[8,9] The <200 fs time constant was attributed to the formation of the retinal excited state, while the 400 fs and 8 ps time constants are identified with multiple excited state decays to the 13-cis photoproduct.[9] The time resolution of our experiment prohibits measurement of a <0.2 ps time constant process. However, the 500−700 fs process in our data appears to correspond to the 400 fs determined from the visible absorption experiments reflecting formation of a red-shifted photointermediate. The absence of a 2 ps ground state recovery component in the ultrafast visible transients may be due to the presence of an overlapping signal from excited state absorption.[8,9] Further experiments are necessary to determine if the components of the 11−12 ps TIR DAS data assigned to chromophore modes are analogous to the 8 ps process attributed to multiple excited state decay in the visible absorption experiments or are simply minor structural changes in the chromophore.

TIR data also show that, concomitant with retinal isomerization, a downshift occurs in frequency of the amide II mode of one or more peptide groups from 1548 cm^{-1} to near 1538 cm^{-1} and is assigned on the basis of total-^{15}N and C15D isotope labeling. This amide II perturbation then relaxes with an ~11−12 ps time constant. The subpicosecond amide II backbone changes may be associated with the storage and transfer of the absorbed photon energy that is eventually used to drive proton transport. For example, photon energy which drives retinal photoisomerization could be transmitted to the Lys-231 peptide group on helix G through structural changes in the Lys-231 side chain, which forms a Schiff base attachment with retinal through the ϵ-nitrogen.[1] This energy could be stored through distortion of the backbone structure around Lys-231 indicated by a downshift of the amide II frequency associated with a weakening of peptide N−H hydrogen bonds.[40] Energy transfer beyond Lys-231 in helix G may also occur through nonlinear excitations similar to those observed in the predominantly α-helical myoglobin.[41] Photon energy could also be transmitted to helix

G through a change in the retinal Schiff base interaction with the Asn-230 side chain deduced using low-temperature FTIR difference spectroscopy and site-directed mutagenesis.[14] In support of this model, the homologous residue, Thr-204 in SRII, is predicted to be involved in the initial energy storage for the purpose of signal transduction.[42]

In BR, evidence for structural changes in the side chain and associated peptide group of the homologous residue Lys-216 in helix G was found by low-temperature (70 K) FTIR difference spectroscopy[43,44] and low-temperature (110−125 K) X-ray crystallography of the trapped K-intermediate.[45] However, a second low-temperature (100 K) X-ray study of the K-intermediate revealed only local changes in the retinal structure which were associated with energy storage.[46] It is worth noting that the rapid structural changes we observe at RT in GPR may be suppressed at low temperature.

Acknowledgment. We thank Jurek Olejnik for synthesis of the C15D labeled retinal and Vladislav Bergo and Jeff Shattuck for helpful discussions. This work was supported by NIH Grant GM069969 to K.J.R., NIH Grant R37GM27750, DOE Grant DE-FG02-07ER15867, and the Robert A. Welch foundation to J.L.S., NSF Grant CHE-0310497 to L.D.Z., and NSF Grant DBI-0242697 and DoD Grant W81XWH-04-1-0578 to S.E.

Supporting Information Available: Figures S1−S3 as defined in the text. This information is available free of charge via the Internet at http://pubs.acs.org.

References and Notes

(1) Beja, O.; Aravind, L.; Koonin, E. V.; Suzuki, M. T.; Hadd, A.; Nguyen, L. P.; Jovanovich, S. B.; Gates, C. M.; Feldman, R. A.; Spudich, J. L.; Spudich, E. N.; DeLong, E. F. *Science* **2000**, *289*, 1902−1906.

(2) Beja, O.; Spudich, E. N.; Spudich, J. L.; Leclerc, M.; DeLong, E. F. *Nature* **2001**, *411*, 786−789.

(3) Rusch, D. B.; Halpern, A. L.; Sutton, G.; Heidelberg, K. B.; Williamson, S.; Yooseph, S.; Wu, D.; Eisen, J. A.; Hoffman, J. M.; Remington, K.; Beeson, K.; Tran, B.; Smith, H.; Baden-Tillson, H.; Stewart, C.; Thorpe, J.; Freeman, J.; Andrews-Pfannkoch, C.; Venter, J. E.; Li, K.; Kravitz, S.; Heidelberg, J. F.; Utterback, T.; Rogers, Y.-H.; Falcon, L. I.; Souza, V.; Bonilla-Rosso, G.; Eguiarte, L. E.; Karl, D. M.; Sathyendranath, S.; Platt, T.; Bermingham, E.; Gallardo, V.; Tamayo-Castillo, G.; Ferrari, M. R.; Strausberg, R. L.; Nealson, K.; Friedman, R.; Frazier, M.; Venter, J. C. *PLoS Biol.* **2007**, *5*, e77.

(4) Spudich, J. L.; Jung, K.-H. Microbial Rhodopsins: Phylogenetic and Functional Diversity. In *Handbook of Photosensory Receptors*; Briggs, W., Spudich, J. L., Eds.; Wiley-VCH: New York, 2005; pp 1−24.

(5) Venter, J. C.; Remington, K.; Heidelberg, J. F.; Halpern, A. L.; Rusch, D.; Eisen, J. A.; Wu, D.; Paulsen, I.; Nelson, K. E.; Nelson, W.; Fouts, D. E.; Levy, S.; Knap, A. H.; Lomas, M. W.; Nealson, K.; White, O.; Peterson, J.; Hoffman, J.; Parsons, R.; Baden-Tillson, H.; Pfannkoch, C.; Rogers, Y. H.; Smith, H. O. *Science* **2004**, *304*, 66−74.

(6) Sabehi, G.; Loy, A.; Jung, K. H.; Partha, R.; Spudich, J. L.; Isaacson, T.; Hirschberg, J.; Wagner, M.; Beja, O. *PLoS Biol.* **2005**, *3*, e273.

(7) Friedrich, T.; Geibel, S.; Kalmbach, R.; Chizhov, I.; Ataka, K.; Heberle, J.; Engelhard, M.; Bamberg, E. *J. Mol. Biol.* **2002**, *321*, 821−838.

(8) Huber, R.; Kohler, T.; Lenz, M. O.; Bamberg, E.; Kalmbach, R.; Engelhard, M.; Wachtveitl, J. *Biochemistry* **2005**, *44*, 1800−1806.

(9) Lenz, M. O.; Huber, R.; Schmidt, B.; Gilch, P.; Kalmbach, R.; Engelhard, M.; Wachtveitl, J. *Biophys. J.* **2006**, *91*, 255−262.

(10) Herbst, J.; Heyne, K.; Diller, R. *Science* **2002**, *297*, 822−825.

(11) Dobler, J.; Zinth, W.; Kaiser, W.; Oesterhelt, D. *Chem. Phys. Lett.* **1988**, *144*, 215.

(12) Mathies, R. A.; Cruz, C. H. B.; Pollard, W. T.; Shank, C. V. *Science* **1988**, *240*, 777−779.

(13) Rothschild, K. J.; Zagaeski, M.; Cantore, W. A. *Biochem. Biophys. Res. Commun.* **1981**, *103*, 483−489.

(14) Bergo, V.; Amsden, J. J.; Spudich, E. N.; Spudich, J. L.; Rothschild, K. J. *Biochemistry* **2004**, *43*, 9075−9083.

(15) Groot, M. L.; van Wilderen, L. J.; Larsen, D. S.; van der Horst, M. A.; van Stokkum, I. H.; Hellingwerf, K. J.; van Grondelle, R. *Biochemistry* **2003**, *42*, 10054−10059.

(16) Kim, S.; Jin, G.; Lim, M. *Bull. Korean Chem. Soc.* **2003**, *24*, 1470−1474.

(17) Stoner-Ma, D.; Jaye, A. A.; Matousek, P.; Towrie, M.; Meech, S. R.; Tonge, P. J. *J. Am. Chem. Soc.* **2005**, *127*, 2864−2865.

(18) Kim, J. E.; Pan, D.; Mathies, R. A. *Biochemistry* **2003**, *42*, 5169−5175.

(19) Diller, R.; Jakober, R.; Schumann, C.; Peters, F.; Klare, J. P.; Engelhard, M. *Biopolymers* **2006**, *82*, 358−362.

(20) Peters, F.; Herbst, J.; Tittor, J.; Oesterhelt, D.; Diller, R. *Chem. Phys.* **2006**, *323*, 109.

(21) Smith, S. O.; Braiman, M. S.; Myers, A. B.; Pardoen, J. A.; Courtin, J. M. L.; Winkel, C.; Lugtenburg, J.; Mathies, R. A. *J. Am. Chem. Soc.* **1987**, *109*, 3108−3125.

(22) Smith, S. O.; Pardoen, J. A.; Lugtenburg, J.; Mathies, R. A. *J. Phys. Chem.* **1987**, *91*, 804−819.

(23) Wang, W. W.; Sineshchekov, O. A.; Spudich, E. N.; Spudich, J. L. *J. Biol. Chem.* **2003**, *278*, 33985−33991.

(24) Nuernberger, P.; Krampert, G.; Brixner, T.; Vogt, G. *Rev. Sci. Instrum.* **2006**, *77*, 083113.

(25) Hamm, P.; Lauterwasser, C.; Zinth, W. *Opt. Lett.* **1993**, *18*, 1943−1945.

(26) Jedju, T. M.; Rothberg, L. *Appl. Opt.* **1988**, *27*, 615−618.

(27) Varo, G.; Brown, L. S.; Lakatos, M.; Lanyi, J. K. *Biophys. J.* **2003**, *84*, 1202−1207.

(28) van Stokkum, I. H. M.; Larsen, D. S.; van Grondelle, R. *Biochim. Biophys. Acta: Bioenerg.* **2004**, *1657*, 82.

(29) Hamm, P. *Chem. Phys.* **1995**, *200*, 415.

(30) Aton, B.; Doukas, A. G.; Callender, R. H.; Becher, B.; Ebrey, T. G. *Biochemistry* **1977**, *16*, 2995−2999.

(31) Rothschild, K. J.; Marrero, H.; Braiman, M.; Mathies, R. *Photochem. Photobiol.* **1984**, *40*, 675−679.

(32) Bernard, M. T.; MacDonald, G. M.; Nguyen, A. P.; Debus, R. J.; Barry, B. A. *J. Biol. Chem.* **1995**, *270*, 1589−1594.

(33) Wang, R.; Sivakumar, V.; Johnson, T. W.; Hastings, G. *Biophys. J.* **2004**, *86*, 1061−1073.

(34) Krebs, R. A.; Dunmire, D.; Partha, R.; Braiman, M. S. *J. Phys. Chem. B* **2003**, *107*, 7877−7883.

(35) Dioumaev, A. K.; Brown, L. S.; Shih, J.; Spudich, E. N.; Spudich, J. L.; Lanyi, J. K. *Biochemistry* **2002**, *41*, 5348−5358.

(36) Polland, H. J.; Franz, M. A.; Zinth, W.; Kaiser, W.; Kolling, E.; Oesterhelt, D. *Biophys. J.* **1986**, *49*, 651−662.

(37) McCamant, D. W.; Kukura, P.; Mathies, R. A. *J. Phys. Chem. B* **2005**, *109*, 10449−10457.

(38) Hasson, K. C.; Gai, F.; Anfinrud, P. A. *Proc. Natl. Acad. Sci. U.S.A.* **1996**, *93*, 15124−15129.

(39) Kobayashi, T.; Saito, T.; Ohtani, H. *Nature* **2001**, *414*, 531.

(40) Bellamy, L. J. *The Infrared Spectra of Complex Molecules*; Chapman and Hall: London, 1968; Vol. 2.

(41) Xie, A.; van der Meer, L.; Hoff, W.; Austin, R. H. *Phys. Rev. Lett.* **2000**, *84*, 5435.

(42) Sudo, Y.; Furutani, Y.; Kandori, H.; Spudich, J. L. *J. Biol. Chem.* **2006**, *281*, 34239−34245.

(43) Gat, Y.; Grossjean, M.; Pinevsky, I.; Takei, H.; Rothman, Z.; Sigrist, H.; Lewis, A.; Sheves, M. *Proc. Natl. Acad Sci. U.S.A.* **1992**, *89*, 2434−2438.

(44) McMaster, E.; Lewis, A. *Biochem. Biophys. Res. Commun.* **1988**, *156*, 86−91.

(45) Edman, K.; Nollert, P.; Royant, A.; Belrhali, H.; Pebay-Peyroula, E.; Hajdu, J.; Neutze, R.; Landau, E. M. *Nature* **1999**, *401*, 822−826.

(46) Schobert, B.; Cupp-Vickery, J.; Hornak, V.; Smith, S.; Lanyi, J. *J. Mol. Biol.* **2002**, *321*, 715−726.